Appendix 1

Sonic speed

The bulk sonic speed (c) through a liquid is calculated from Equation A1:

$$\frac{1}{c^2} = \frac{\rho}{K} - \frac{\rho T \alpha^2}{\rho C_V + K T \alpha^2} \quad \text{(A1)}$$

where K is the isothermal bulk modulus ($\equiv 1/\beta_T$) (Ghiorso and Kress 2004). Figure A1a shows the speed of sound through liquid $NaAlSi_3O_8$ is largely P-dependent. Generally, c monotonically increases from about 2000 m/s at 1 bar to 7000 m/s near 30 GPa. The most rapid increase in c with P occurs at P < ~8 GPa. An apparent T-dependence in the c-P slope can be seen at high P, with higher T isotherms exhibiting steeper slopes (Figure A1a).

Grüneisen parameter

The Grüneisen parameter (γ), useful in relating thermoelastic properties at high P and high T, can be defined thermodynamically by Equation A2:

$$\gamma = \frac{\alpha V}{\beta_T C_V} \quad \text{(A2)}$$

(Vočadlo et al. 2000). For liquid $NaAlSi_3O_8$, γ increases monotonically with P at all T of interest (Figure A1b). There is a stronger P-dependence on γ below 2 GPa than at higher P. A crossover point exists around 18.4 GPa, through which all isotherms pass at ~0.82 (Figure A1b). Below 18.4 GPa, γ increases with T at fixed P, and the pattern reverses at higher P.

References for appendix 1

Ghiorso, M.S., and Kress, V.C. (2004) An equation of state for silicate melts. III. Calibration of volumetric properties at 10^5 Pa. American Journal of Science, 304, 679-751.

Vočadlo, L., Poirer, J.P., and Price, G.D. (2000) Grüneisen parameters and isothermal equations of state. American Mineralogist, 85, 390-395.

Appendix 2

Kinks in polyhedra fractions at 4242 K

Figures 8b and 9b (for 4242 ± 19 K) of the main text show kinks near 15 GPa for the fraction curves of SiO_4, SiO_5, AlO_4, and AlO_6 (as well as in some of the minor polyhedra). We compared these fractions to the T-P relationship of the 4242 ± 19 K pseudo-isotherm (see Figure A2). Values of P along the target isotherm are known to within 0.29 GPa. The T (changing with P along the pseudo-isotherm) shows a minimum at 13.6 GPa, corresponding to the kinks in the SiO_4 and SiO_5 polyhedra fraction curves (Figure A2). For Al-O, the kinks in Figure 9b seem to be either concave at 13.6 or convex at 16.5 GPa, corresponding to a local T minimum (4222 K) or an "average" T (4247 K), respectively. It should be noted that the T minimum at 13.6 GPa is less extreme than the minima seen at 1.7 and 7.0 GPa (Figure A2). The T minimum at 1.7 GPa correlates with the polyhedra maxima of AlO_4 and SiO_4; this is a consistent relationship between T and the extrema in fractions of SiO_4 but is inconsistent with those of AlO_4. Additionally, the T minimum at 7.0 GPa is the most extreme, yet fractions in polyhedra show no kink patterns near this P. Although the T values from the simulations (for the 4200 K target isotherm) deviate from the averaged value (4242 K), the standard deviation in T does not explain the kinks in polyhedra fractions.

Another comparison was made with E from the simulation output (EA-1), which has a minimum (along the 4242 ± 19 K pseudo-isotherm) at 13.6 GPa. The E minimum at 13.6 GPa is very shallow, dropping ~0.1% between the adjacent values. This correlates with kinks in Si-O polyhedra but is less convincing for Al-O fractions. From these observations, it is not clear that the E extrema is large enough to influence the polyhedra statistics.

Diffusivities were also analyzed with the coordination fractions. D_{Na} makes a very slight concave up shape at 13.6 GPa, which corresponds to the (convex) kink in SiO_4 fraction. This relationship may suggest that Na mobility decreases due to the increase in polymerization (where 4-fold coordination implies a tetrahedron structure and thus a more polymerized network) and decrease in the size of pathways through the structure. However, this relationship is not the same for AlO_4 abundances, and no other atom type exhibits a prominent feature in self-diffusion near 15 GPa. Thus, we conclude that diffusivity has little influence on the 15 GPa kinks in polyhedra fractions.

Appendix 3

Polyhedra equilibria

To further investigate the connection between thermodynamics and short-range liquid structure, we developed a thermodynamic equilibria model using the coordination statistics on Si-O, Al-O, and O-Si polyhedra. This simple model can be used to predict (to first-order approximation) the dependence of polyhedra abundances as a function of P and T over the P-T range of the MD simulations. Following the procedure in Morgan and Spera (2001), the method incorporates stepwise polyhedral equilibria and the law of mass action. For example, the concentrations of SiO_4, SiO_5, and SiO_6 are related via the equilibrium reaction

$$SiO_4^{-4} + SiO_6^{-8} \rightleftharpoons 2SiO_5^{-6}, \quad \text{(A3)}$$

for which the change in Gibbs energy (ΔG) is zero at equilibrium. That is,

$$\Delta G(P,T) = 0 = \Delta H^\circ(T) - T\Delta S^\circ(T) + \int_{P^\circ}^{P} \Delta V(P,T)\,dP + RT \ln\left[\frac{a_{SiO_5}^2}{a_{SiO_4} a_{SiO_6}}\right] \quad \text{(A4)}$$

where P° is a reference pressure, and H, S, and a represent enthalpy, entropy, and the activity, respectively. We assume that

the change in isobaric heat capacity (ΔC_P) is zero, the change in volume (ΔV) of the reaction is constant, and the polyhedra mix ideally. Based on these assumptions, Equation A4 reduces to

$$\Delta G(P,T) = 0 = \Delta H^\circ - T\Delta S^\circ + \Delta V(P - P^\circ) + \mathrm{R}T \ln\left[\frac{x_{\mathrm{SiO_5}}^2}{x_{\mathrm{SiO_4}} x_{\mathrm{SiO_6}}}\right] \quad \text{(A5)}$$

with ΔH, ΔS, and ΔV remaining constant, and X representing number fractions from the coordination statistics of the corresponding polyhedra.

We used multiple linear regression models to extract values of ΔH, ΔS, and ΔV from Equation A5 for four polyhedra reactions. In addition to the SiO_5 polyhedra reaction (Equation A3), the following equilibria were analyzed:

$$\mathrm{AlO_4^{-5}} + \mathrm{AlO_6^{-9}} \rightleftharpoons 2\mathrm{AlO_5^{-7}} \quad \text{(A6)}$$

$$\mathrm{OSi_0^{-2}} + \mathrm{OSi_2^{+6}} \rightleftharpoons 2\mathrm{OSi_1^{+2}} \quad \text{(A7)}$$

$$\mathrm{OSi_1^{+2}} + \mathrm{OSi_3^{+10}} \rightleftharpoons 2\mathrm{OSi_2^{+6}}. \quad \text{(A8)}$$

Equations A6–A8 have the same form as that of Equation A3 and thus, under the same assumptions, follow the same development as Equation A5.

The thermodynamic parameters obtained from this analysis are collected in Table A1. All four polyhedra equilibrium regressions had an R^2 statistic above 0.88. Despite the approximations that (1) ΔH and ΔS for the reactions are independent of T, (2) ΔV of the reactions is constant and independent of P and T, and (3) mixing of polyhedra is ideal, the abundances of the various polyhedra are remarkably well recovered for a large span in P (~0–30 GPa) and T (~3100–5100 K) using the parameters of Table A1. This simple thermodynamic model shows promise for future MD studies of liquid structure as a means to quantify thermodynamic equilibria parameters.

REFERENCES FOR APPENDIX 3

Morgan, N.A., and Spera, F.J. (2001) A molecular dynamics study of the glass transition in $CaAl_2Si_2O_8$: Thermodynamics and tracer diffusion. American Mineralogist, 86, 915-926.

Tables for appendices

Table A1. Thermodynamic parameters from the polyhedral equilibria (Equation A5).

Equilibrium reaction[a]	ΔS (J mol^{-1} K^{-1})	ΔV (m^3/mol)	ΔH (J/mol)	R^2
Eq. A3	12.95	-1.122E-07	7262.70	0.9669
Eq. A6	6.27	-2.484E-07	-12602.73	0.9089
Eq. A7	15.44	4.273E-07	-3402.29	0.9753
Eq. A8	5.96	1.380E-06	-82905.91	0.8860

[a] Equation number referenced in Appendix 3.

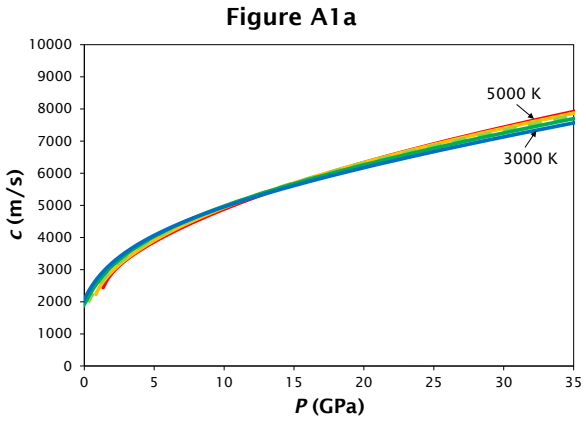

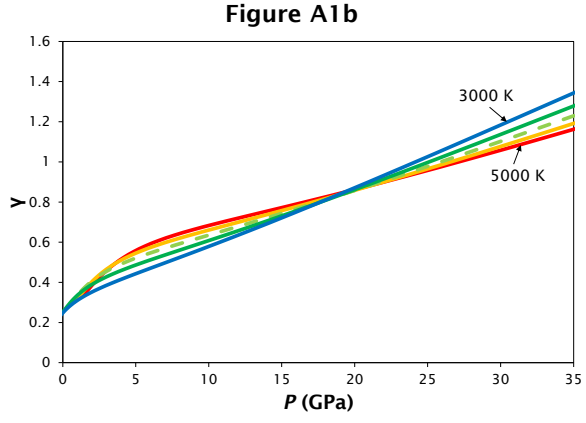

FIGURE A1. Additional thermodynamic properties from the EOS analysis. Both panels use the same five isothermal curves: 3000, 3500, 4000, 4500, and 5000 K. The dashed line represents 4000 K. (**a**) Sonic speed versus *P*. (**b**) The Grüneisen parameter versus *P*. Note the crossover point near 18.4 GPa (see Appendix 1 text).

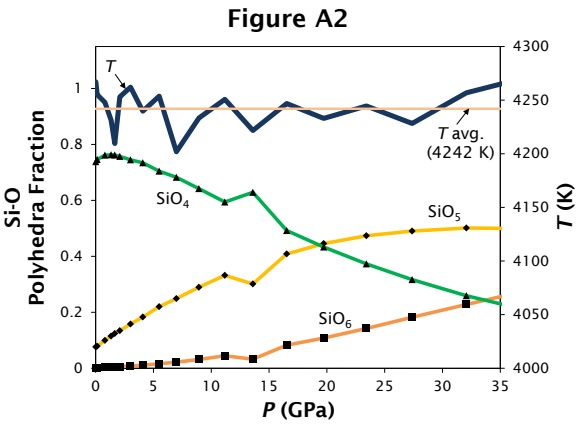

FIGURE A2. *T* variations along the 4242 ± 19 K pseudo-isotherm from the MD simulations, overprinted onto the Si-O polyhedra coordination fractions (compare to Figure 8b in the text). Polyhedra fractions for SiO_3 are not drawn for clarity. Horizontal line indicates the average *T* (4242 K) from the 19 simulations with target *T* of 4200 K.